

## THE UNUSUAL *SPITZER* SPECTRUM OF THE CARBON STAR IRAS 04496–6958: A DIFFERENT CONDENSATION SEQUENCE IN THE LMC?

ANGELA K. SPECK

Department of Physics and Astronomy, University of Missouri, Columbia, MO 65211; speckan@missouri.edu

JAN CAMI

SETI Institute, NASA Ames Research Center, MS 245-6, Moffett Field, CA 94035-1000

ČISKA MARKWICK-KEMPER AND JARRON LEISENRING

Department of Astronomy, University of Virginia, P.O. Box 400325, Charlottesville, VA 22904-4325

RYSZARD SZCZERBA

Nicolaus Copernicus Astronomical Center, Polish Academy of Sciences, Radańska 8, 87-100 Toruń, Poland

CATHARINUS DIJKSTRA

Department of Physics and Astronomy, University of Missouri, Columbia, MO 65211

SCHUYLER VAN DYK

*Spitzer* Science Center, California Institute of Technology, MC 220-6, Pasadena, CA 91125

AND

MARGARET MEIXNER

Space Telescope Science Institute, 3700 San Martin Drive, Baltimore, MD 21218

*Received 2006 April 22; accepted 2006 June 9*

### ABSTRACT

We present a new *Spitzer* Infrared Spectrograph (IRS) spectrum of the carbon star IRAS 04496–6958 in the Large Magellanic Cloud, which exhibits a fairly broad absorption feature at  $\sim 11 \mu\text{m}$ . This feature is consistent with SiC absorption, as seen in a few Galactic sources. Furthermore, the  $\text{C}_2\text{H}_2$  (and other molecular) absorption bands are the deepest ever observed, indicative of a very high column density. While the Galactic sources with SiC absorption have cool colors (continuum temperature  $\approx 300 \text{ K}$ ), IRAS 04496–6958 is much bluer, with a continuum temperature of  $\approx 600 \text{ K}$ . Based on the Galactic sample, SiC dust at this temperature should still display an emission feature at  $\sim 11 \mu\text{m}$ . If SiC is the cause of the absorption feature, it suggests a subtly different evolutionary path and a change to a different condensation sequence than assumed for Galactic carbon stars. An alternative explanation for this feature is molecular line absorption; however, currently available line lists are not sufficient to properly assess this hypothesis.

*Subject headings:* circumstellar matter — dust, extinction — infrared: stars — stars: carbon — stars: individual (IRAS 04496–6958)

### 1. INTRODUCTION

Stars in the mass range  $1\text{--}8 M_\odot$  eventually evolve up the asymptotic giant branch (AGB; Iben & Renzini 1983), where they begin to lose mass and form circumstellar shells of dust and gas. During their ascent of the AGB, mass-loss rates are expected to increase with the luminosity of the star, resulting in progressive optical thickening of circumstellar shells. Furthermore, the chemistry of these stars' atmospheres, and thus of their circumstellar shells, changes as a result of the dredge-up of newly formed carbon from the He-burning shell. Due to the extreme ease of formation and stability of CO molecules, the chemistry in circumstellar shells is controlled by the C/O ratio. If  $\text{C/O} < 1$ , then all the carbon is trapped in CO, leaving oxygen to dominate the chemistry. Conversely, if  $\text{C/O} > 1$ , then all the oxygen is trapped in CO, and carbon dominates the chemistry. Stars start their lives with cosmic C/O ratios ( $\approx 0.4$ ) and are thus oxygen-rich. In some AGB stars, the dredge-up of newly formed carbon is efficient enough to raise the C/O above unity, and these stars are known as carbon stars. They are expected to have circumstellar shells dominated by amorphous or graphitic carbon grains, although other dust grains are also important (e.g., silicon carbide [SiC]). Consequently, the spectra of carbon stars are expected to be dom-

inated by a featureless continuum with some contribution at  $\sim 11 \mu\text{m}$  from SiC.

As the mass-loss rate increases with the evolution of the AGB stars, these stars eventually become invisible at optical wavelengths and very bright in the infrared (IR). Such stars are known as “extreme carbon stars” (Volk et al. 1992, 2000). At this stage, intense mass loss depletes the remaining hydrogen in the star's outer envelope and terminates the AGB. Up to this point the star has been making and dredging up carbon; thus, these shells have even more carbon available for dust production than optically bright (early) carbon stars (i.e., the Si/C ratio decreases with the evolution of these stars).

Here we examine the case of IRAS 04496–6958 in the Large Magellanic Cloud (LMC), which was classified as an obscured AGB star by Zijlstra et al. (1996). Trams et al. (1999) investigated the *Infrared Space Observatory* Camera (ISOCAM) Continuous Variable Filter (CVF) spectrum of IRAS 04496–6958 and found an apparent silicate emission feature. Unfortunately, their spectrum only covered a limited wavelength range ( $\sim 6\text{--}15 \mu\text{m}$ ). As shown in § 3, this apparent silicate emission is an artifact of the underestimation of the level of the continuum emission. This misidentification occurred because of the unprecedentedly strong acetylene ( $\text{C}_2\text{H}_2$ ) absorption features exhibited

in this star’s spectrum. Thus, IRAS 04496–6958 is not a silicate carbon star, and silicate carbon stars remain a Galactic phenomenon. Nonetheless, Trams et al. (1999) suggested that the silicate feature is further evidence of hot bottom burning (HBB), which would increase the nitrogen abundance and suppress carbon production.

Matsuura et al. (2005) investigated the  $3\ \mu\text{m}$  spectra of AGB stars in nearby galaxies. The strengths of the observed  $\text{C}_2\text{H}_2$  features implies a C/O ratio  $>1.4$  (cf. an average of C/O = 1.1 for Galactic carbon stars). Furthermore, investigation of the strength of the HCN features suggests that there are two populations of carbon stars in the LMC: strong HCN and weak HCN. For IRAS 04496–6958 the HCN is clearly detected and falls into the strong HCN category, indicating that nitrogen is not underabundant in this object. However, the HCN feature only requires the nitrogen abundance to scale with the carbon and does not need to be overabundant. Thus, in disagreement with Trams et al. (1999), HBB is not necessary for this object.

In § 2 we present the new *Spitzer Space Telescope* Infrared Spectrograph (IRS; Houck et al. 2004) spectrum of IRAS 04496–6958. In § 3 we compare this spectrum to the spectra of Galactic extreme carbon stars and to model spectral energy distributions (SEDs). In § 4 we discuss the cause of this odd spectrum. The summary and conclusions are in § 5.

## 2. OBSERVATIONS AND DATA REDUCTION

IRAS 04496–6958 was observed on 2004 March 1 with IRS on board the *Spitzer Space Telescope* (Werner et al. 2004; PID: 1094; AOR Key: 9069312), in IRS staring mode, using both the low spectral resolution (Short-Low and Long-Low;  $R \approx 60$ –125;  $5$ – $40\ \mu\text{m}$ ) and the high-resolution modules (Short-High only;  $R \approx 600$ ;  $9.9$ – $19.3\ \mu\text{m}$ )

We obtained the Basic Calibrated Data (BCD) products from pipeline S13 from the *Spitzer* archive. These BCDs are images to which only the most basic calibration steps are applied, and several additional steps were required to complete the data reduction process. First, we used the image masks to identify the bad pixels and replaced them with the average value of the surrounding 8 pixels. We thus correct for saturation and nonlinear behavior of the pixels in the BCD. For the low-resolution data, we corrected  $\leq 4\%$  of the pixels; for the high-resolution data, the number of corrected pixels was closer to 10%. Then, we subtracted the background or sky emission for the low-resolution data using the off-nod positions. From the resulting images the subspectra were subtracted using the SMART data reduction package (Higdon et al. 2004), where the extraction column was selected close to the centroid of the collapsed spectrum (4.046 pixels wide in SMART units). The width of the extraction column depends on the wavelength, correlated with the size of the point-spread function. The same procedure was applied to spectra of calibration star  $\alpha$  Lac to obtain the spectra. Using a template for  $\alpha$  Lac available through the *Spitzer* Science Center<sup>1</sup> (see also Cohen et al. 2003), we have calibrated the relative flux levels of the low- and high-resolution spectra of IRAS 04496–6958. All the orders were scaled to match the flux levels measured with the short-wavelength module of the low-resolution spectra. The errors in the fluxes are approximated 2%–3% for the low-resolution data and 5%–10% for the high-resolution data.

## 3. ANALYSIS OF THE SPECTRUM OF IRAS 04496–6958

Figure 1 shows the spectrum of IRAS 04496–6958 with the best-fit blackbody (600 K). We attempted to fit this spectrum

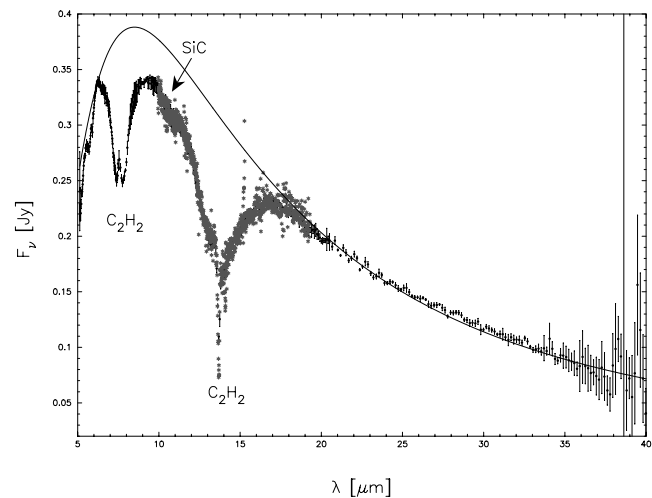


FIG. 1.—*Spitzer* IRS spectrum of IRAS 04496–6958 together with best-fit blackbody continuum (600 K; solid line). Black points are low-resolution IRS spectrum (Short-Low and Long-Low) and include error bars; gray asterisks are high-resolution IRS spectrum (Short-High only); errors are not shown, but are typically 5%–10%.

using a modified blackbody<sup>2</sup> with index of the emissivity law varying from 1 to 2, but we were unable to match the long-wavelength tail of the emission distribution. It is clear in this figure that there must be something absorbing in the  $11\ \mu\text{m}$  region to account for the dip in intensity between the  $\text{C}_2\text{H}_2$  molecular absorptions at  $\sim 7$  and  $13.7\ \mu\text{m}$ . While blackbody fits to the continuum probably exaggerate the amount of absorption around  $11\ \mu\text{m}$ , even the “conservative” continuum, from more detailed radiative transfer modeling of the SED (see § 3.2), shows an absorption around  $11\ \mu\text{m}$ .

The cause of this absorption is not known. While it is possible that molecular absorptions could explain this broad absorption feature, cool SiC grains in the outer circumstellar regions are a good candidate.

### 3.1. Observing Dust around Carbon Stars

Circumstellar shells of carbon stars are expected to be dominated by amorphous or graphitic carbon grains. These dust species do not have diagnostic IR features and merely contribute to the dust continuum emission. However, silicon carbide (SiC) exhibits a strong IR feature at  $\sim 11\ \mu\text{m}$ . SiC has been of great interest to stardust researchers, since its formation was predicted by condensation models for carbon-rich circumstellar regions (Gilman 1969; Friedemann 1969 and references therein). Following these predictions, a broad IR emission feature at  $\sim 11.4\ \mu\text{m}$  has been observed in the spectra of many carbon stars and is attributed to solid SiC particles (e.g., Hackwell 1972; Treffers & Cohen 1974).

The effect of dust shell evolution on observed spectral features, and particularly on the  $\sim 11\ \mu\text{m}$  feature, have been discussed extensively (e.g., Speck et al. 2005 and references therein). All studies concur that the increasing optical depth leads to decreasing color temperatures from these stars as the stellar photosphere becomes hidden from view, and the dust from which we receive light becomes progressively cooler. At the same time, the  $\sim 11\ \mu\text{m}$  feature tends to become weaker (relative to the continuum) and flatter topped (less sharp peaked) and possibly broader. Various explanations of this behavior have been proposed, but none are

<sup>1</sup> See [http://ssc.spitzer.caltech.edu/irs/calib/templ/cohen\\_models/](http://ssc.spitzer.caltech.edu/irs/calib/templ/cohen_models/).

<sup>2</sup> We used  $F(\lambda) \propto B(\lambda, T)\lambda^{-\beta}$ , where  $\beta$  is the index of emissivity law.

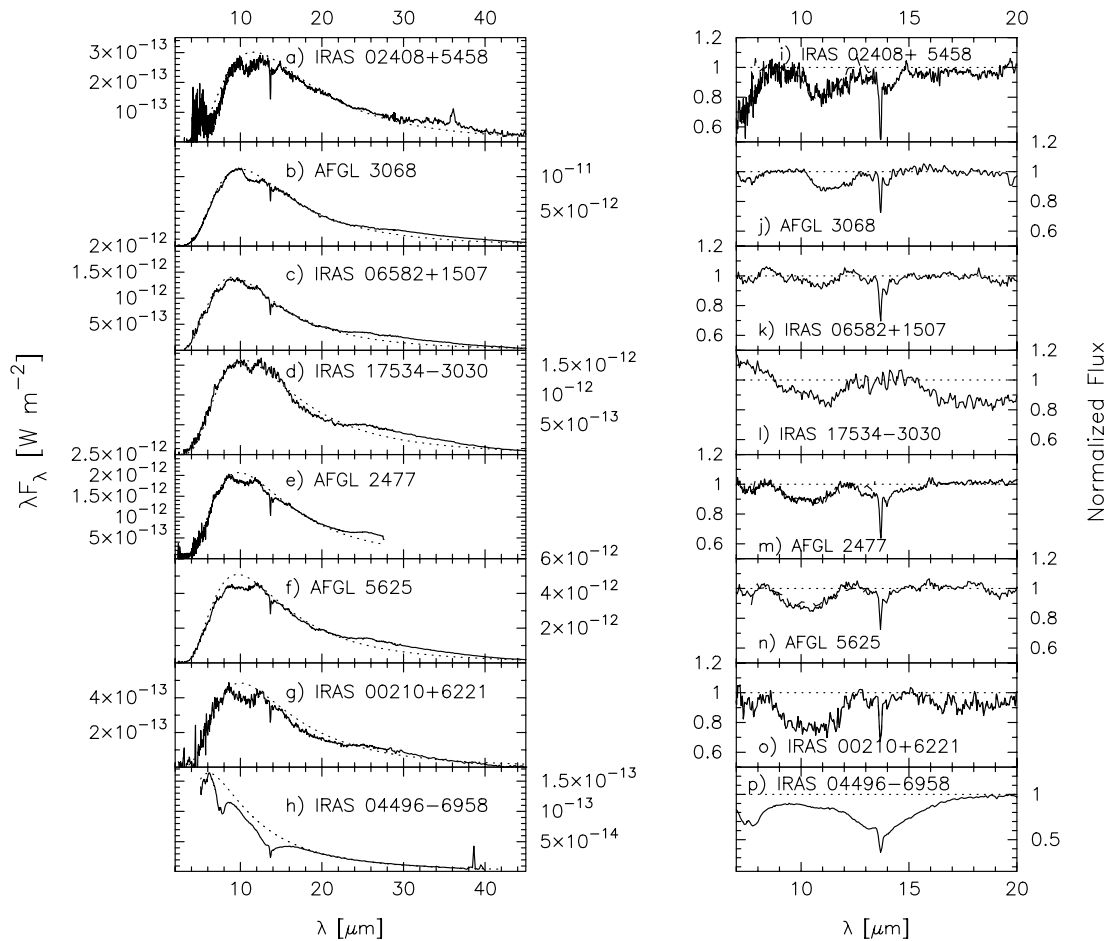


FIG. 2.—*ISO* SWS spectra of seven Galactic extreme carbon stars compared with *Spitzer* IRS low-resolution spectrum of IRAS 04496–6958. *Left*: Flux-calibrated spectra (solid lines) together with best-fit blackbodies (dotted lines). *Right*: Continuum-divided spectra (solid lines) and continuum level (dotted lines). For detailed information on observations and data reduction for *ISO* SWS spectra, see Speck et al. (2005) and Pitman et al. (2006).

entirely satisfactory. Initially the diminution of the  $\sim 11 \mu\text{m}$  feature was attributed to coating of the grains by amorphous carbon (e.g., Baron et al. 1987; Chan & Kwok 1990). However, meteoritic data do not support this hypothesis (Bernatowicz et al. 2006; Clayton & Nittler 2004 and references therein). Presolar SiC grains are almost never found with a carbon coating. Moreover, more recent studies of the  $\sim 11 \mu\text{m}$  feature have shown that it is consistent with SiC self-absorption, i.e., absorption by cooler SiC particles, located in the outer part of the dust shell, where they can absorb the SiC emission feature produced by warmer SiC closer to the central star (Speck et al. 1997). As the dust shell reaches extreme optical depths, the  $\sim 11 \mu\text{m}$  feature will eventually be seen in net absorption. However, these absorption features are rare and have mostly been ignored in discussions of evolutionary sequences for carbon star spectra.

### 3.1.1. Comparison of Carbon Star $11 \mu\text{m}$ Absorption Features

Figure 2 shows the comparison of the IR spectrum IRAS 04496–6958 with those of Galactic extreme carbon stars. The broad SiC absorption seen in AFGL 5625, AFGL 2477, and IRAS 00210+6221 matches the position and depth of the feature needed to account for  $11 \mu\text{m}$  absorption seen in IRAS 04496–6958. Speck et al. (2005) attributed this broad feature to amorphous SiC with C impurities (see § 4.1).

There is an obvious difference between the LMC spectrum and the Galactic spectra that exhibit this  $11 \mu\text{m}$  absorption feature. While the Galactic sources have continuum temperatures

around 300 K, the continuum temperature of IRAS 04496–6958 is  $\sim 600$  K. Galactic carbon stars with such high continuum temperatures exhibit SiC emission features. However, even for such Galactic carbon stars, SiC absorption is occurring, leading to weaker emission features. Speck et al. (1997) showed that every star in their sample whose underlying continuum temperature was below 1200 K was best fitted by self-absorbed SiC, whether the  $\sim 11 \mu\text{m}$  feature was in net emission or net absorption. In this case, the inner SiC closest to the star produces an emission feature. The outer dust is cool enough to absorb this feature, reducing its strength (the emission feature is self-absorbed), but the absorption is not strong enough to produce a net absorption feature. A logical explanation for the IRAS 04496–6958 spectrum is that we are seeing SiC absorption of a featureless continuum, i.e., the inner dust does not produce an  $11 \mu\text{m}$  emission feature. This is shown schematically in Figure 3. Such a scenario would imply that early mass loss from carbon stars leads to the formation of SiC grains, while later mass loss either does not form SiC or the SiC grains are effectively hidden by thick carbon mantles. If this is the case, then it is clear that this carbon star in the LMC is exhibiting evidence for a different condensation sequence to Galactic carbon stars.

### 3.2. Modeling of SiC Absorption Features

In order to test the hypothesis that the  $\sim 11 \mu\text{m}$  absorption is due to cool SiC in the outermost regions of the circumstellar shells, we have employed radiative transfer modeling. For this

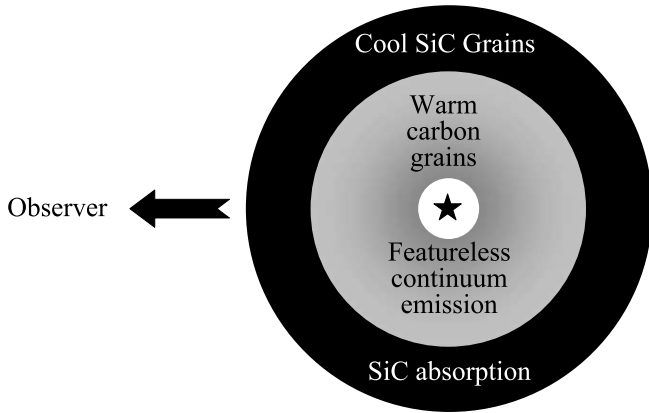


FIG. 3.—Schematic cartoon of dust shell structure.

purpose the numerical code described in Szczerba et al. (1997) has been used with optical constants for amorphous carbon (AC cel 800 sample) from Jäger et al. (1998), from which absorption and scattering AC efficiencies have been computed by means of the Mie theory. The widely applied optical constants for AC from Rouleau & Martin (1991) cannot be used for this purpose, since they show nonsmooth behavior around 10–12  $\mu\text{m}$ , probably due to the presence of carbon in nonamorphous forms and/or Si impurities. We modeled the dust shell using a Mathis-Rumpl-Nordsieck (MRN)-like<sup>3</sup> grain size distribution and obtained a fairly good fit to the SED of IRAS 04496–6859, assuming that the central source has  $T_{\text{eff}} = 2500$  K and  $L/d^2 = 590 L_{\odot} \text{ kpc}^{-2}$ . This implies a very high luminosity (about 30,000  $L_{\odot}$  at distance of the LMC). The fit is shown in both panels of Figure 4 by thick

<sup>3</sup> We used  $n(a) \propto a^{-q}$ , where  $n$  is the number of grains in the size interval  $(a, a + da)$  and  $q = 3.5$ ,  $a_{\text{min}} = 0.005$  and  $a_{\text{max}} = 0.25 \mu\text{m}$  (Mathis et al. 1977).

solid lines, while the input blackbody spectrum of the central star is shown by thick dashed lines. The IRS spectrum of IRAS 04496+6859 is represented by shorter thin solid lines in  $10^{-10} \text{ ergs cm}^{-2} \text{ s}^{-1}$  (*top*) and in janskys (*bottom*). The fit required an outer radius to be only  $5 \times 10^{16}$  cm (an inner radius of dust shell coincides with a dust temperature of 1000 K) and density distribution proportional to  $r^{-1.55}$ . This suggests that the mass-loss rate was decreasing as a function of time (at least during the last 1500 yr necessary to fill up the shell with typical velocity of 10  $\text{km s}^{-1}$ ), and assuming a dust-to-gas ratio of 0.01 implies a mass loss of  $2.85 \times 10^{-6}$  and  $3.39 \times 10^{-7} M_{\odot} \text{ yr}^{-1}$  at the outer and inner radius of the shell, respectively. However, such a conclusion is not necessarily true. The required density distribution depends strongly on the spectral slope of dust opacity in the mid-IR. For the AC cel 800 sample used here, the spectral index in the range between 10 and 40  $\mu\text{m}$  is about  $-1.21$ . Taking dust with smaller index (e.g.,  $-2$ , which is typical for more ordered forms of dust) the required density distribution would be more steep, suggesting different behavior of mass loss (even increasing with time). The remaining model parameters of the shell are: total visual extinction  $A_V = 4.8$ , dust mass of  $3.11 \times 10^{-5} M_{\odot}$ , and the mean dust temperature at the outer radius of about 126 K.

The fit shown in Figure 4 represents more conservative continuum estimation than that from blackbody fitting shown in Figure 1. However, the absorption around 11  $\mu\text{m}$  is still clearly seen as shown in Figure 5, which shows a close-up of the mid-IR portions of both panels from Figure 4. The solid lines are the same as in Figure 4, while dashed lines now represent the model spectrum seen through a slab of SiC dust. We have used SiC optical constants from Pégourié (1988) and the Mie theory to compute the extinction coefficient. We find that additional extinction  $A_V \lesssim 0.5$  is enough to get the absorption feature around 11  $\mu\text{m}$ .

The modeling results suggest that SiC grains existing at distances larger than  $5 \times 10^{16}$  cm will have temperatures  $\lesssim 100$  K.

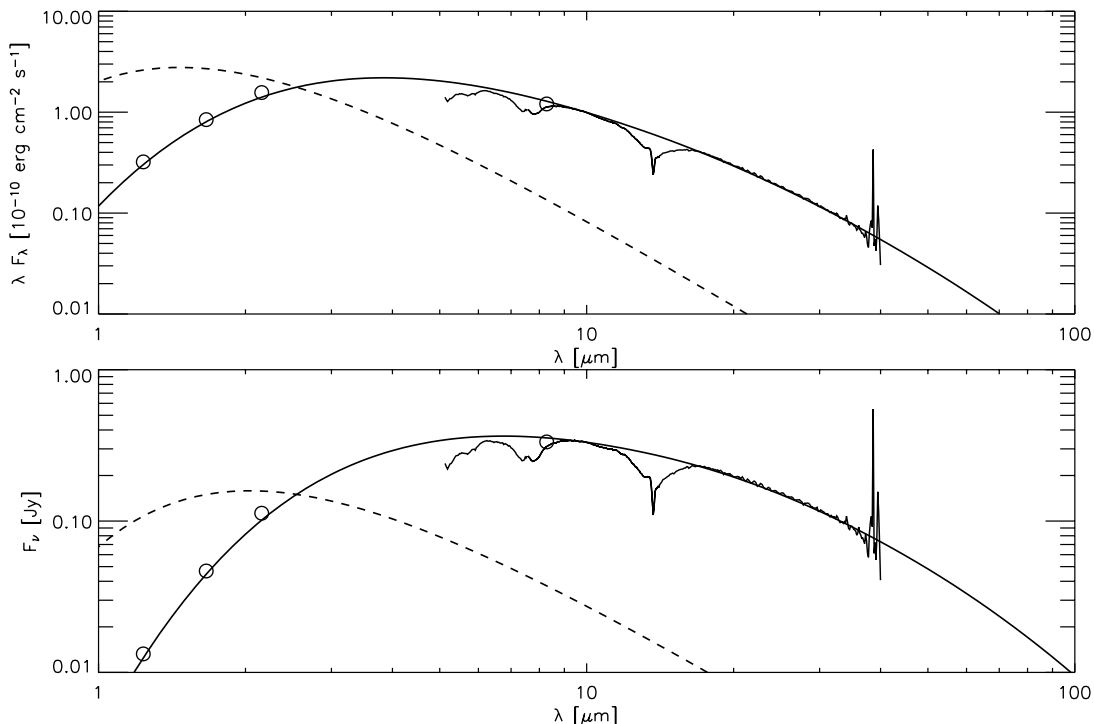


FIG. 4.—Model fits to the continuum of IRAS 04496–6958. Thin solid lines are the IRS spectrum, thick dashed lines are the stellar continuum, and thick solid lines are the model fit. Circles are the  $J$ ,  $H$ ,  $K$  photometry from the Two Micron All Sky Survey (Kleinmann et al. 1994) and  $A$  band at 8.28  $\mu\text{m}$  from the *Midcourse Space Experiment* (Price et al. 2001). The  $x$ -axis is log wavelength in microns. *Top*:  $y$ -axis in  $\lambda F_{\lambda}$ . *Bottom*:  $y$ -axis is  $F_{\nu}$  in janskys.

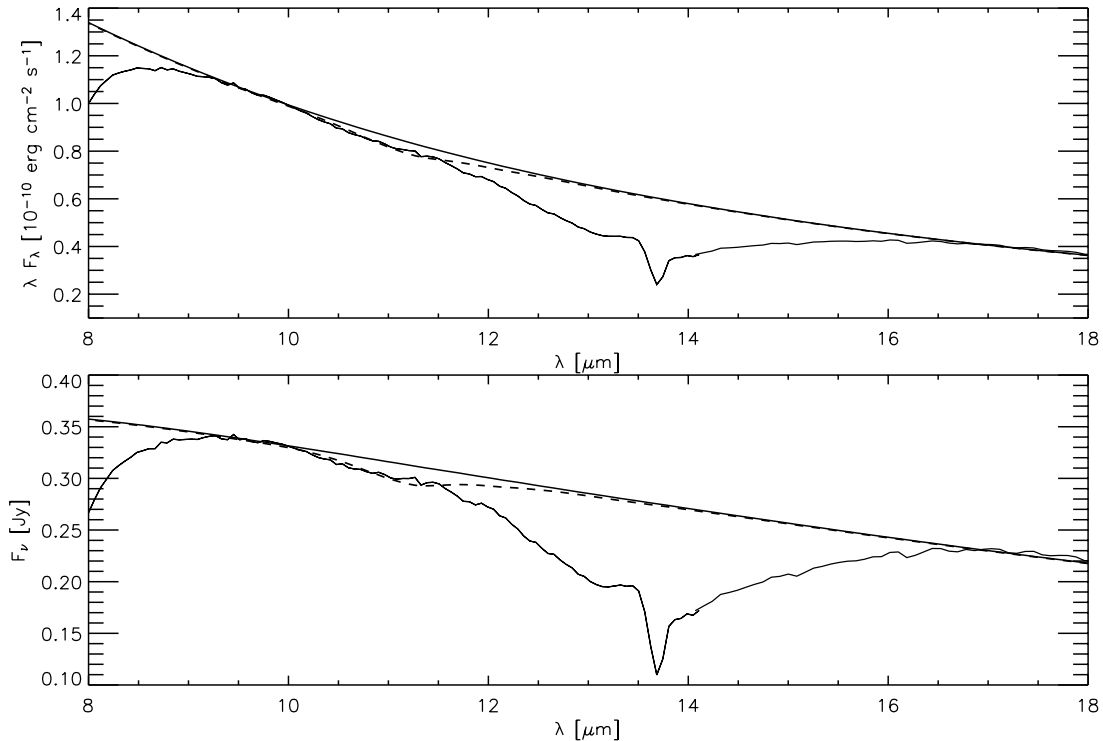


FIG. 5.—Model fits to the continuum of IRAS 04496–6958: Close-up of 8–18  $\mu\text{m}$  region. The thin lines are the IRS spectrum; the thick solid lines show the continuum fit from radiative transfer modeling using AC only; and the dashed lines show spectrum seen through SiC with  $A_V = 0.5$ , which corresponds to  $A_{11.3}$  of about 0.1. *Top*: y-axis in  $\lambda F_\lambda$ . *Bottom*: y-axis is  $F_\nu$  in janskys.

At this temperature emission will contribute mainly in 20–30  $\mu\text{m}$  range, with much smaller contribution around 11–13  $\mu\text{m}$ . Therefore, absorption at  $\sim 11$   $\mu\text{m}$  should be seen.

While numerous radiative transfer models of carbon stars have been published previously (e.g., Rowan-Robinson & Harris 1983; Chan & Kwok 1990; Lorenz-Martin & Lefèvre 1993, 1994; Groenewegen 1995; Blanco et al. 1998), very few of these modeling efforts have been aimed at these extreme carbon stars with absorption features in the 8–13  $\mu\text{m}$  range. Furthermore, most previous models assume that the SiC and AC grains are cospatial and share the same inner dust radius/temperature. Volk et al. (1992) modeled the SEDs for six Galactic extreme carbon stars and found IR optical depths in the range  $1.5 < \tau_{11.3 \mu\text{m}} < 7.9$ , visual extinctions in the range  $86 < A_V < 900$ , and luminosities in the range  $472 < L_*/D^2 < 9420$ . Groenewegen et al. (1998) modeled 44 carbon stars, but only three fall in the extreme carbon star category, and of those, only two show an apparent SiC absorption feature (AFGL 3068 and AFGL 190). Their models are consistent with those of Volk et al. (1992). The model dust mass-loss rates were found to be  $(5.5\text{--}9.5) \times 10^{-7} M_\odot \text{ yr}^{-1}$ . Interestingly, these models use little or no SiC (<8% SiC by mass). Volk et al. (2000) modeled the *ISO* spectra of five extreme C stars (one of which still shows SiC in emission). Their models consisted of AC dust and an empirical 30  $\mu\text{m}$  feature. No attempt was made to fit the absorption features in the  $\sim 11$   $\mu\text{m}$  region. For the stars in their sample with SiC absorption features, IR optical depths are in the range  $2.1 < \tau_{11.3 \mu\text{m}} < 4.5$ , visual extinctions are in the range  $260 < A_V < 550$ , and luminosities are in the range  $450 < L_*/D^2 < 2143$ . In contrast to our models, Volk et al. (2000) found that the density distribution varies as  $r^{-\alpha}$ , where  $2.25 < \alpha < 3$ , but used Rouleau & Martin (1991) optical constants for AC. As discussed above, the precise spectral slope of the dust opacity is critical in determining the radial density distribution. Previous

models have much higher visual extinctions than our model for IRAS 04496–6958; however, this is to be expected. IRAS 04496–6958 is more similar to an “average,” mildly self-absorbed Galactic carbon that still exhibits a SiC feature in emission (e.g., IRAS 05373–0810 and IRAS 03488+3943; Szczerba et al. [2002] and Groenewegen et al. [1998], respectively). The absorption feature occurs in this less extreme environment due to a change in the condensation sequence (see § 4.2).

### 3.3. Spectral Contributions from Molecular Gas

The spectrum of IRAS 04496–6958 shows many clear molecular absorption bands. The most notable is a deep and broad absorption band between 11 and 17  $\mu\text{m}$ , with the deepest absorption at 13.7  $\mu\text{m}$ . A second clear absorption band is between 6.5 and 8.5  $\mu\text{m}$ , and additional absorption bands are present shortward of 6  $\mu\text{m}$ .

#### 3.3.1. The 11–17 $\mu\text{m}$ Absorption Band

The deepest part of the absorption at 13.7  $\mu\text{m}$  corresponds to the *Q*-branch of the  $\nu_5$  antisymmetric bending mode ( $729 \text{ cm}^{-1}$ ) of  $\text{C}_2\text{H}_2$  (acetylene). It is interesting to note that the entire molecular absorption band has quite an extraordinary width. Depending on the choice of continuum, this band starts at about 10–11.5  $\mu\text{m}$  and ends at about 17  $\mu\text{m}$ . In this entire range, only two fundamental transitions of  $\text{C}_2\text{H}_2$  exist: the *trans*- and *cis*-bending modes at  $611 \text{ cm}^{-1}$  (16.4  $\mu\text{m}$ ) and  $729 \text{ cm}^{-1}$  (13.7  $\mu\text{m}$ ), respectively. If the entire absorption band is due to  $\text{C}_2\text{H}_2$ , this then indicates that the wings of the absorption are due to contributions from *P*- and *R*-branch transitions arising from high rotational *J*-levels, and/or from hot bands and combination bands in this wavelength range. In turn, to have an observable population in these levels, this indicates either warm material or large column densities (or both). However, since the dust continuum

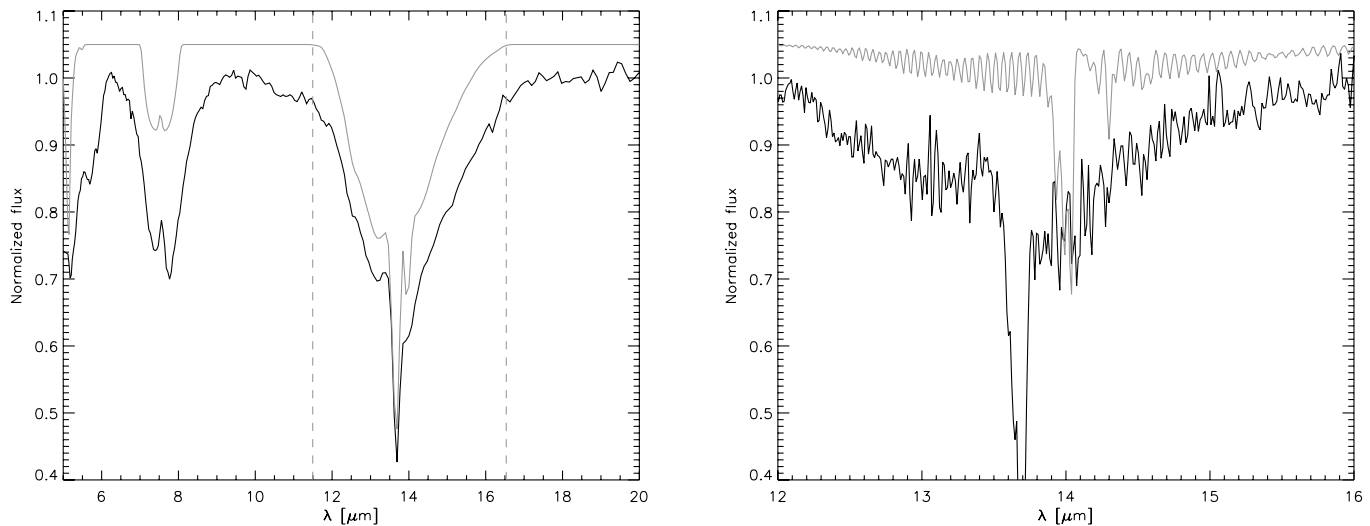


FIG. 6.—*Left*: Five-layer LTE slab model using the HITRAN line list for acetylene. The vertical dashed lines indicate the limits of the HITRAN line list for the fundamental bending modes and various hot bands. The black line is the IRS low-resolution spectrum; the gray line is the model. *Right*: Model for HCN absorption near the fundamental  $\nu_2$  bending mode. The presence of HCN cannot be unambiguously established from the absorption in this range. The black line is IRS high-resolution spectrum; the gray line is the model. High-frequency structure in the models are due to  $P$ - and  $R$ -branch lines. Models are offset for clarity.

closely resembles a 600 K blackbody, and we see the molecular bands in absorption, the excitation temperatures of the molecular layers must be lower than 600 K. Therefore, if the entire molecular absorption is due to  $C_2H_2$ , then the column densities must indeed be very high ( $\lesssim 5 \times 10^{20} \text{ cm}^{-2}$ ).

This high column density makes it almost impossible to produce a good fit with existing line data on the acetylene transitions. The latest HITRAN<sup>4</sup> line list (Rothman et al. 2005) contains transitions in the range  $604\text{--}870 \text{ cm}^{-1}$  ( $11.5\text{--}16.5 \mu\text{m}$ ) and lists transitions with  $J \leq 50$ . Clearly, this will make it impossible to reproduce the entire absorption band with only this line list; moreover, excitation temperatures and column densities derived from using this line list will not be very reliable. As an example, we show in Figure 6 a model using the HITRAN line list. Whereas the main  $Q$ -branch band is reasonably well fitted, the structure in the wings

is not, and the observed absorption clearly extends beyond the limits in the line list (*dashed lines*). Also, the absorption band between  $6.5$  and  $8.5 \mu\text{m}$  is not well reproduced at all. This wavelength range contains many overtones and combination bands of the two bending modes, but other molecules may contribute as well (see below).

In this wavelength range, there might also be a contribution due to HCN, which has its  $\nu_2$  bending mode at  $712 \text{ cm}^{-1}$  ( $14.05 \mu\text{m}$ ). However, as can be seen from Figure 6, HCN can only play a modest role in explaining the broad and deep absorption. Indeed, even when ignoring the absorption of acetylene at the wavelength of the strongest HCN absorption, it is seen that HCN can at most modestly produce absorption in this range. And while there are some coincidences with small spectral features in the observed spectrum and a model spectrum for HCN, the observations do not show convincing evidence for HCN absorption. HCN should furthermore also produce notable absorption around  $7 \mu\text{m}$  (see Fig. 7). While HCN might contribute to absorption in the

<sup>4</sup> High-resolution Transmission molecular absorption database.

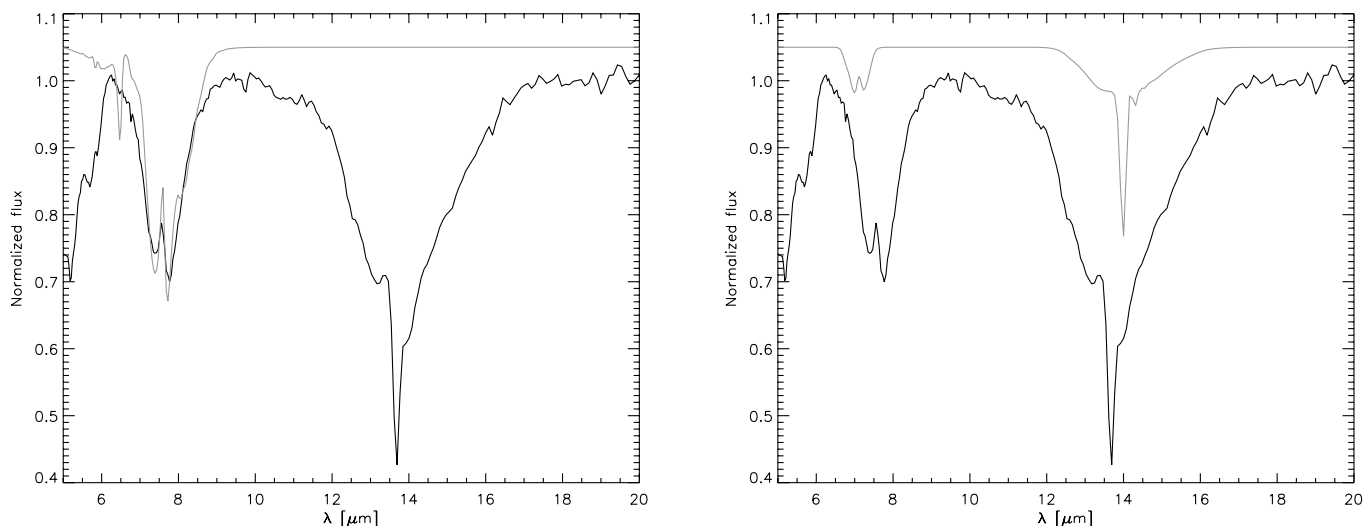


FIG. 7.—*Left*: Methane absorption model for the band between  $6.5$  and  $8.5 \mu\text{m}$ . *Right*: Illustration of HCN absorption. Black lines are IRS low-resolution spectrum; gray lines are the models. Models are offset for clarity.

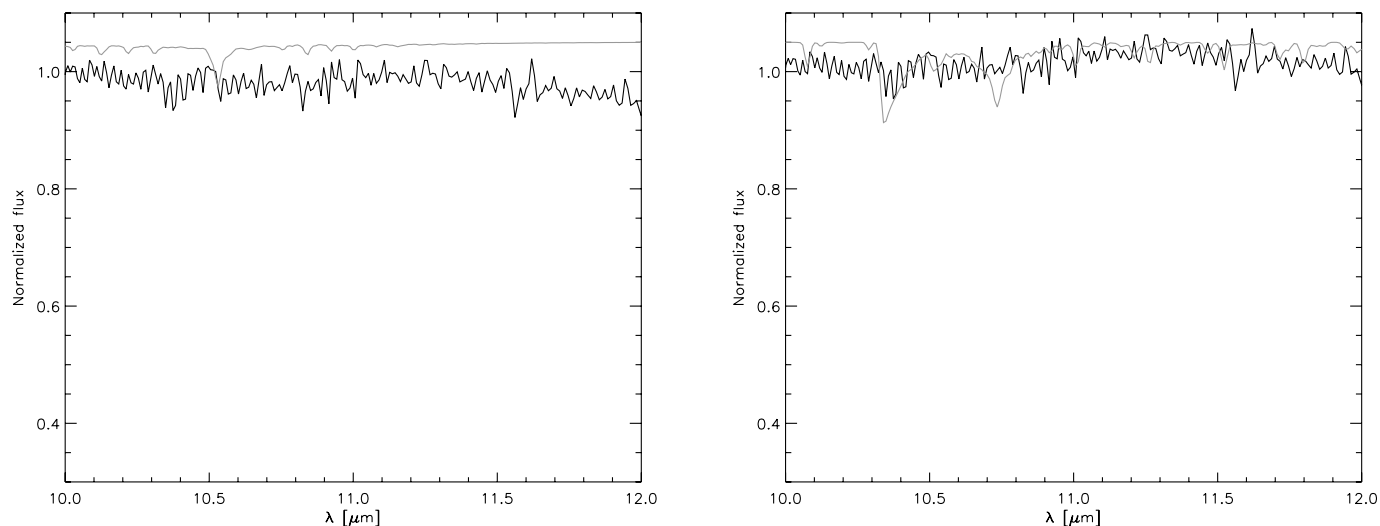


FIG. 8.—*Left:*  $C_2H_4$  absorption model between 10 and 12  $\mu m$ . *Right:*  $NH_3$  absorption model in the same wavelength range. Black lines are IRS high-resolution spectrum; gray lines are the models. Models are offset for clarity.

wings of the 6.5–8.5  $\mu m$  absorption band, it can at most be a small contribution.

### 3.3.2. The 6.5–8.5 $\mu m$ Band

As can be seen from Figure 6, acetylene also produces absorption in 6.5–8.5  $\mu m$  wavelength range (Zijlstra et al. 2006). However, also in this range, the HITRAN line list seems highly insufficient to reproduce the observed absorption. It is unclear whether this is only due to the limited number of transitions in the line list, or whether other molecules might be absorbing too. For instance, methane ( $CH_4$ ) has a triply degenerate  $\nu_4$  bending mode at  $1306\text{ cm}^{-1}$  (7.66  $\mu m$ ), which also might well be contributing to this band (see Fig. 7).

### 3.3.3. Other Possible Molecular Bands in the 10–12 $\mu m$ Region

In this range, there are many other molecules that might produce detectable absorption. Carbon stars in which  $C_2H_2$  is detected often also exhibit the lines of  $C_2H_4$ . In addition,  $NH_3$  has some strong transitions in this wavelength range. For these molecules, the line lists present in HITRAN are even more limited than those of  $C_2H_2$ , and therefore again, a good model fit is impossible. Figure 8 shows some examples using  $C_2H_4$  and  $NH_3$  models in the 10–12  $\mu m$  region. Again, the presence of these molecules cannot be unambiguously corroborated from the observations, but they might play a role in explaining the absorption observed in this wavelength range. There are many other molecules that have transitions in this range (e.g.,  $C_3$ ; Zijlstra et al. 2006; Jørgensen et al. 2000), but their line lists are not readily available. Furthermore, the theoretical spectrum of  $C_3$  from Jørgensen et al. (2000) shows a strong absorption close to the  $\sim 5\text{ }\mu m$  CO line, which is stronger than the  $\sim 11\text{ }\mu m$  feature. While it is difficult to determine the presence/absence of this feature in IRS data, it is not seen in the *ISO* spectra of Galactic carbon stars (AFGL 5625, AFGL 2477, and IRAS 00210+8221) that exhibit this broad  $\sim 11\text{ }\mu m$  spectral feature.

## 4. DISCUSSION

### 4.1. The SiC Absorption Feature

The prototype for extreme carbon stars is the Galactic star AFGL 3068, which has an absorption feature at  $\sim 11\text{ }\mu m$ , tentatively attributed to absorption by SiC (Jones et al. 1978).

Speck et al. (1997) reinvestigated AFGL 3068 and confirmed this absorption feature. In addition, Speck et al. (1997) discovered three more extreme carbon stars (IRAS 02408+5458, AFGL 2477, and AFGL 5625) with  $\sim 11\text{ }\mu m$  absorption features, attributable to SiC. Two of these objects (AFGL 2477 and AFGL 5625) exhibit a broader absorption feature, with the  $\sim 11\text{ }\mu m$  feature extended on the blue side. Speck et al. (1997) attributed this shorter wavelength contribution to interstellar silicate absorption along the line of sight in addition to the SiC  $\sim 11\text{ }\mu m$  absorption feature.

The absorption features of AFGL 3068 and IRAS 02408+5458 were revisited by Clément et al. (2003), who showed that these features, as seen in *ISO* Short Wavelength Spectrometer (SWS) spectra, were consistent with isolated  $\beta$ -SiC nanoparticles (confirming the results of Speck et al. [1999]). However, they could not fit the short-wavelength side of the  $\sim 11\text{ }\mu m$  absorption feature using SiC alone, which may indicate that this “blue” absorption is intrinsic to these stars and that its strength varies.

The broad absorption features of AFGL 2477 and AFGL 5625 were revisited by Clément et al. (2005). This work presented new IR spectra of silicon nitride ( $Si_3N_4$ ) and found a correlation between the observed broad feature and the laboratory absorption spectrum. Furthermore, they correlated various weaker longer wavelength absorptions in the astronomical spectra, with those of  $Si_3N_4$  observed in the laboratory. However, the match to the longer wavelength features is dubious ( $< 2\sigma$ ; Pitman et al. 2006). Furthermore, in the laboratory spectra the relative strengths of the features in the  $\sim 9$ –12  $\mu m$  region compared to the longer wavelength features indicates that  $Si_3N_4$  cannot be solely responsible for the broad  $\sim 11\text{ }\mu m$  absorption feature. Moreover,  $Si_3N_4$  is not predicted to form in the circumstellar shells of carbon stars unless they have an extreme overabundance of nitrogen ( $> 100$  times solar; Lodders & Fegley 1995), and presolar  $Si_3N_4$  grains do not originate from AGB stars (Amari et al. 2002).

Speck et al. (2005) showed that three more extreme carbon stars exhibit absorption features similar to those discussed above (see Fig. 2). It is clear that IRAS 06582+1507 shows the  $\sim 11\text{ }\mu m$  absorption feature seen in AFGL 3068 and IRAS 02408+5458. The spectrum of IRAS 00210+6221 shows a broad feature similar to that of AFGL 5625 and AFGL 2477. IRAS 17534–3030 seems to be intermediate between the two. These newly discovered  $\sim 11\text{ }\mu m$  absorption features suggest that there is a continuum

of similar features with FWHM ranging from  $\sim 2$  to  $\sim 2.8 \mu\text{m}$ . This trend from narrow to broad features has been interpreted either as a dust sequence from relatively pure crystalline  $\beta$ -SiC to increasingly amorphous SiC grains with carbon impurities (Speck et al. 2005) or as relatively pure crystalline  $\beta$ -SiC with increasing contributions from  $C_3$  (Zijlstra et al. 2006).

#### 4.2. Theoretical Models of Carbon Star Dust Condensation

In order to explain the proposed changes in dust condensation sequence (see § 3.1.1), we need to consider how dust condensation may be different in the lower metallicity (and possibly more carbon-rich) environment in the LMC.

There have been many studies of the expected condensation sequence in Galactic carbon stars. These studies showed how the condensation sequence of carbon (C), titanium carbide (TiC), and SiC is dependent on various parameters, including C/O ratio, gas pressure, and N abundance (Lodders & Fegley 1995; Sharp & Wasserburg 1995). Gas pressure is a measure of the mass-loss rate (together with the photospheric temperature and outflow velocity). Sharp & Wasserburg (1995) found that graphite (carbon) condensation temperature ( $T_{\text{cond}}$ ) is strongly dependent on C/O, while the  $T_{\text{cond}}$  for TiC and SiC are not. Conversely, the condensation temperature of carbon is more or less independent of gas pressure, but  $T_{\text{cond}}$  for TiC and SiC varies strongly with gas pressure. However, Lodders & Fegley (1995) found that C, TiC, and SiC are all strongly dependent on both gas pressure and C/O ratio. In presolar grains TiC is found in the center of carbon grains from AGB stars, but only one SiC grain has been found coated in carbon (Clayton & Nittler 2004; Bernatowicz et al. 2006). Sharp & Wasserburg (1995) argued that if carbon forms at a higher condensation temperature, closer to the star than SiC, then there is a significant decrease in the amount of carbon available in the gas, and thus SiC and carbon (C) do not form simultaneously, resulting in naked SiC grains. Therefore, for Galactic sources, the condensation sequence in the majority of carbon stars should be TiC–C–SiC, in order to produce coated TiC grains and uncoated (naked) SiC grains.

Observational evidence for naked SiC grains is discussed by Speck et al. (2005). Sharp & Wasserburg (1995) argued that from kinetic and stellar model considerations, dust grains should form in the pressure range  $2 \times 10^{-7} < P < 4 \times 10^{-5}$  bars.<sup>5</sup> Therefore, to form dust in the sequence TiC–C–SiC, they need  $1.04 < C/O < 1.2$ . For Galactic carbon stars the C/O ratio is expected to be in the range 1–1.8, with a mean C/O ratio of  $\sim 1.15$  (Lambert et al. 1986; Olofsson et al. 1993a, 1993b).

Lodders & Fegley (1995) also modeled the effect of C/O and pressure on the condensation sequence in carbon stars, as well as the effect of *s*-process and nitrogen abundances. They also briefly discussed the effect of metallicity. The general trends in condensation temperatures are: (1) all condensation temperatures decrease as the gas pressure decreases, and (2) at  $C/O > 1$  the  $T_{\text{cond}}$  of graphite increases with C/O (for a given pressure and otherwise constant composition).

In their solar metallicity models we see that for low C/O ( $\leq 1.5$ ) C only forms before SiC for low pressures. At high pressures SiC will form first. For solar metallicity and  $C/O = 1.05$ , SiC forms before carbon for  $P \geq 3.4 \times 10^{-5}$  bars. As C/O increases, the minimum pressure required to form SiC first increases such that at  $C/O = 1.2$ ,  $P \geq 10^{-3}$  bars. Above  $C/O \sim 1.5$  carbon always forms before SiC. The exact C/O ratio at which the carbon forms before

SiC depends on pressure. Therefore, in order to account for observations of SiC features in the Galaxy, and the presolar grain record, we can restrict the *P*-C/O space such that, for low C/O the gas pressure must remain low, but for higher C/O the pressure can be higher. This can be used to constrain the dust-forming environment around Galactic carbon stars.

For IRAS 04496–6958, we need to look at the effect of metallicity. With decreasing metallicity the condensation temperatures tend to decrease, but the effect is stronger for carbon than for SiC. For example, at  $P = 10^{-5}$  bars and solar abundance, C condenses at 1646 K, and SiC condenses at 1546 K, leading to naked SiC grains. However, for the same pressure and a metallicity of  $[\text{metals}/\text{H}] = -1$ , carbon condenses at 1436 K, and SiC condenses at 1460 K. In this case SiC forms before carbon, and thus SiC will be coated in a mantle of carbon. The condensation sequence is always sensitive to the gas pressure and the C/O ratio, so that even at low metallicity it is possible to form C before SiC. The effect of a smaller change in metallicity, relevant to the LMC ( $[\text{metals}/\text{H}] = -0.3$ ), is not known, but we assume the trends hold.

During the AGB phase, the circumstellar region becomes progressively C-rich (increasing C/O due to dredge-up of C from the He-burning shell). Meanwhile, the mass-loss rate is expected to increase, leading to an increase in the gas pressure. For solar composition carbon stars start with low C/O and low *P*. As time goes on both increase, but in order to match the observations of SiC features and the evidence from presolar grains, the C/O must go up fast enough with the increasing pressure to prevent the formation of SiC before C in the majority of carbon stars. For the lower metallicity environment, however, at a given C/O ratio, a lower pressure is required in order for SiC to form before C. Carbon stars in the LMC reach mass-loss rates similar to those found in the Galaxy (Matsuura et al. 2005; Van Loon et al. 1999). Based on the similar mass-loss rates and stellar temperatures for LMC and Galactic carbon stars (Van Loon et al. 1999), we expect the gas pressure around LMC carbon stars to be comparable to the Galactic carbon stars. But the critical pressure at which SiC can form before C decreases with metallicity. Therefore, even with similar stars and similar mass-loss rates to Galactic sources, the condensation sequence may change. In the early stages of a carbon star's life, the pressure and C/O ratio are both low, and C forms before SiC. As the C/O and mass loss (gas pressure) increase, SiC can form before C, even at a gas pressure where this would not happen for higher metallicities. This would tend to change the dust condensation sequence as the star evolves such that early dust formation would follow the sequence TiC–C–SiC, while later dust formation may follow TiC–SiC–C. In this case, a carbon star can have cool naked SiC absorbing the continuum emission from warm carbon (and carbon-coated SiC) in the inner part of the dust shell (see Fig. 3).

At high C/O carbon will always form before SiC, negating this compositional radial structure for the dust shell. So what C/O ratios do we expect for the LMC, and how does that relate to IRAS 04496–6958? The average C/O ratio for carbon stars in the LMC appears to be somewhat higher than in the Galaxy ( $> 1.4$  LMC vs. 1.15 Galactic; Matsuura et al. 2005). For this C/O and solar metallicity, the gas pressure required to form SiC before C is high, but not unrealistic.

Another issue is the effect of nitrogen abundance. Lodders & Fegley (1995) investigated the effect of increasing the nitrogen abundance (relative to solar). Decreasing N abundances tend to increase the  $T_{\text{cond}}$  for all carbon-bearing condensates. Lower nitrogen abundances tend to make it easier to form carbon before SiC. If the nitrogen abundance in IRAS 04496–6958 is much

<sup>5</sup> The expected range of gas pressures in the dust formation zone for O-rich AGB stars in the LMC is  $10^{-7}$  bars  $\lesssim P \lesssim 10^{-4}$  bars (Dijkstra et al. 2005).

lower than solar, the C/O ratio will need to be reduced and gas pressure increased in order to be able to form SiC before carbon. Detailed models showing the effects of metallicity and nitrogen abundance are not currently available. Matsuura et al. (2005) detected a strong HCN feature in the 3  $\mu\text{m}$  spectrum of IRAS 04496–6958, implying that the N abundance scales as carbon (i.e., nitrogen abundance is neither particularly low nor particularly high.)

All of the Galactic extreme carbon stars for which *ISO* spectra exist exhibit the 26–30  $\mu\text{m}$  feature attributed to magnesium sulfide (MgS; Volk et al. 2000; Hony et al. 2002). This feature is not evident in the spectrum of IRAS 04496–6958. Lodders & Fegley (1995) found that for MgS the  $T_{\text{cond}}$  depends on the total pressure in the gas, but not on the C/O ratio. MgS will form at much lower temperatures than the major C-bearing condensates (C and SiC). A possible explanation for the lack of MgS emission may be that by the time the temperature has dropped to the condensation temperature, the density is so low as to inhibit formation. This may also explain the paucity/weakness of MgS 30  $\mu\text{m}$  features observed in the Small Magellanic Cloud (SMC; Sloan et al. 2006).

## 5. CONCLUSIONS

We have shown that the *Spitzer* spectrum of IRAS 04496–6958 shows no evidence for a silicate emission. Furthermore,

this spectrum is consistent with absorption by cool SiC in the outer regions of the circumstellar shell. While the strong molecular absorption bands may support a molecular origin, current line lists are unable to reproduce this absorption feature. Furthermore, the nature of the spectrum suggests that there is a change in the condensation sequence in carbon stars in the LMC that is not seen in Galactic carbon stars. Whereas Galactic sources always produce SiC grains that are naked, the LMC stars begin making naked SiC grains, but later in their evolution the LMC stars produce grains that are coated in the much more abundant carbon condensates. This scenario may also explain the weakness of the SiC emission features seen in the LMC (Zijlstra et al. 2006) and SMC (Sloan et al. 2006). This observation can be used to constrain the progressing mass-loss rates and C/O ratios in LMC carbon stars needed to see the change in condensation sequence.

A. K. S. and C. D. are supported in part by the NASA Astrophysical Data Program (NAG5-12675) and the University of Missouri Research Board. R. S. has been supported by grant 2.P03D 017.25 of the Polish State Committee for Scientific Research. M. M. is supported by NASA NAG5-12595.

## REFERENCES

- Amari, S., Jennings, C., Nguyen, A., Stadermann, F. J., Zimmer, E., & Lewis, R. S. 2002, *Lunar Planet. Sci. Conf.*, 33, 1205
- Baron, Y., de Muizon, M., Papoular, R., & Pégourié, B. 1987, *A&A*, 186, 271
- Bernatowicz, T. J., et al. 2006, in *Meteorites and the Early Solar System II*, ed. D. Lauretta & H. Y. McSween, Jr. (Tucson: Univ. Arizona Press), 109
- Blanco, A., Borghesi, A., Fonti, S., & Orofino, V. 1998, *A&A*, 330, 505
- Chan, S. J., & Kwok, S. 1990, *A&A*, 237, 354
- Clayton, D. D., & Nittler, L. R. 2004, *ARA&A*, 42, 39
- Clément, D., Mutschke, H., Klein, R., & Henning, T. 2003, *ApJ*, 594, 642
- Clément, D., Mutschke, H., Klein, R., Jäger, C., Dorschner, J., Sturm, E., & Henning, T. 2005, *ApJ*, 621, 985
- Cohen, M., Megeath, S. T., Hammersley, P. L., Martín-Luis, F., & Stauffer, J. 2003, *AJ*, 125, 2645
- Dijkstra, C., Speck, A. K., Reid, R. B., & Abraham, P. 2005, *ApJ*, 633, L133
- Friedemann, C. 1969, *Physica*, 41, 189
- Gilman, R. C. 1969, *ApJ*, 155, L185
- Groenewegen, M. A. T. 1995, *A&A*, 293, 463
- Groenewegen, M. A. T., Whitelock, P. A., Smith, C. H., & Kerschbaum, F. 1998, *MNRAS*, 293, 18
- Hackwell, J. A. 1972, *A&A*, 21, 239
- Higdon, S. J. U., et al. 2004, *PASP*, 116, 975
- Hony, S., Waters, L. B. F. M., & Tielens, A. G. G. M. 2002, *A&A*, 390, 533
- Houck, J. R., et al. 2004, *ApJS*, 154, 18
- Iben, I., Jr., & Renzini, A. 1983, *ARA&A*, 21, 271
- Jäger, C., Mutschke, H., & Henning, Th. 1998, *A&A*, 332, 291
- Jones, B., Merrill, K. M., Puetter, R. C., & Willner, S. P. 1978, *AJ*, 83, 1437
- Jørgensen, U. G., Hron, J., & Loidl, R. 2000, *A&A*, 356, 253
- Kleinmann, S. D., et al. 1994, *Ap&SS*, 217, 11
- Lambert, D. L., Gustafsson, B., Eriksson, K., & Hinkle, K. H. 1986, *ApJS*, 62, 373
- Lodders, K., & Fegley, B., Jr. 1995, *Meteoritics*, 30, 661
- Lorenz-Martin, S., & Lefèvre, J. 1993, *A&A*, 280, 567
- . 1994, *A&A*, 291, 831
- Mathis, J. S., Rimpl, W., & Nordsieck, K. H. 1977, *ApJ*, 217, 425
- Matsuura, M., et al. 2005, *A&A*, 434, 691
- Olofsson, H., Eriksson, K., Gustafsson, B., & Carlstrom, U. 1993a, *ApJS*, 87, 267
- . 1993b, *ApJS*, 87, 305
- Pégourié, B. 1988, *A&A*, 194, 335
- Pitman, K., Hofmeister, A. M., & Speck, A. K. 2006, *MNRAS*, in press
- Price, S. D., Egan, M. P., Carey, S. J., Mizuno, D. R., & Kuchar, T. A. 2001, *AJ*, 121, 2819
- Rothman, L. S., et al. 2005, *J. Quant. Spectrosc. Radiat. Transfer*, 96, 139
- Rouleau, F., & Martin, P. G. 1991, *ApJ*, 377, 526
- Rowan-Robinson, M., & Harris, S. 1983, *MNRAS*, 202, 797
- Sharp, C. M., & Wasserburg, G. J. 1995, *Geochim. Cosmochim. Acta*, 59, 1633
- Sloan, G. C., et al. 2006, *ApJ*, 645, 1118
- Speck, A. K., Barlow, M. J., & Skinner, C. J. 1997, *MNRAS*, 288, 431
- Speck, A. K., Hofmeister, A. M., & Barlow, M. J. 1999, *ApJ*, 513, L87
- Speck, A. K., Thompson, G. D., & Hofmeister, A. M. 2005, *ApJ*, 634, 426
- Szczerba, R., Chen, P. S., Szymczak, M., & Omont, A. 2002, *A&A*, 381, 491
- Szczerba, R., Omont, A., Volk, K., Cox, P., & Kwok, S. 1997, *A&A*, 317, 859
- Trams, N. R., et al. 1999, *A&A*, 344, L17
- Treffers, R., & Cohen, M. 1974, *ApJ*, 188, 545
- van Loon, J., et al. 1999, *A&A*, 351, 559
- Volk, K., Kwok, S., & Langill, P. P. 1992, *ApJ*, 391, 285
- Volk, K., Xiong, G.-Z., & Kwok, S. 2000, *ApJ*, 530, 408
- Werner, M. W., et al. 2004, *ApJS*, 154, 1
- Zijlstra, A., et al. 1996, *MNRAS*, 279, 32
- . 2006, *MNRAS*, 370, 1961